CrossMark

Fish Heat Shock Cognate 70 Derived AMPs *Cs*HSC70 A1 and *Cs*HSC70 A2

Akila Sathyamoorthi[1,2] · Rajesh Palanisamy[1] · Mariadhas Valan Arasu[3] ·
Naif Abdullah Al-Dhabi[3] · Mukesh Pasupuleti[4] · Jesu Arockiaraj[1]

Abstract Heat shock cognate 70 (HSC70) is an important evolutionary conserved protein that plays a major role in maintaining the homeostasis and immunity of many organisms. In this study, a HSC70 from *Channa striatus* was identified from its cDNA library and characterized using bioinformatics and molecular biology tools. *Cs*HSC70 cDNA was 1953 base pair (bp) in length along with an open reading frame which encoded a polypeptide of 650 amino acid residues. Tissue distribution results showed that *Cs*HSC70 was considerably expressed in gill, to a lesser extent in head kidney, blood, spleen and liver and at low level in other tissues. Using *C. striatus* gill as cell model, effects of fungal, bacterial and poly I:C stimulant on the mRNA levels of *Cs*HSC70 was examined. We also described the antimicrobial features of two peptides namely *Cs*HSC70 A1and *Cs*HSC70 A2 derived from the N-terminal of *Cs*HSC70 protein. *Cs*HSC70 A1 peptide (40 μg/ml) exhibited potent bactericidal activity against *Micrococcus luteus* cells. Flow cytometric analysis revealed that the *M. luteus* cells stained with propidium iodide, upon treated with *Cs*HSC70 A1 at the concentration of 40 μM/ml showed 38% survival compared to its control (99.6%). It seems that *Cs*HSC70 A1 peptide shows antimicrobial activity against *M. luteus* through membrane disruption. Additionally, scanning electron microscope (SEM) observation confirmed that *Cs*HSC70 A1 peptide treatment completely damaged and destructed the *M. luteus* cells. Taken together, these findings suggest that *Cs*HSC70 A1 peptide could be a safe and potential therapeutic molecule substitute to antibiotics in various clinical fields.

Keywords Heat shock cognate · Antimicrobial peptides · Membrane disruption · Hemolysis · Bactericidal

✉ Jesu Arockiaraj
  jesuaraj@hotmail.com

1 Division of Fisheries Biotechnology and Molecular Biology, Department of Biotechnology, Faculty of Science and Humanities, SRM University, Kattankulathur, Chennai, Tamil Nadu 603 203, India

2 Department of Biotechnology, SRM Arts and Science College, Kattankulathur, Chennai 603 203, India

3 Addiriyah Chair for Environmental Studies, Department of Botany and Microbiology, College of Science, King Saud University, P. O. Box 2455, Riyadh 11451, Saudi Arabia

4 Lab PCN 206, Microbiology Division, CSIR-Central Drug Research Institute, B.S. 10/1, Sector 10, Jankipuram Extension, Sitapur Road, Lucknow, Uttar Pradesh 226 031, India

Introduction

Heat shock proteins (HSPs) are an evolutionarily conserved multi-gene encoded family of molecular chaperon proteins and found in many living organisms from bacteria to mammals. They play a major role in maintenance of the cellular protein homeostasis by protecting cells from a wide variety of environmental and physiological stresses, including thermal shock, oxygen radicals, heavy metals, nutrient deprivation, microbial infections, ischemia, heavy metal ions, ethanol, nicotine and surgical stress (Roberts et al. 2010; Yamashita et al. 2010). On the basis of sequence conservation and molecular size, HSPs are grouped into HSP100, HSP90, HSP70, HSP60 and low molecular weight HSP families (Roberts et al. 2010).

Among the family of heat shock proteins, the HSP70 is known to be most abundant and conserved. HSP70s are highly induced in response to a wide variety of physiological and environmental stress. However, even without stress, eukaryotic cells contain high levels of structurally related heat shock cognate proteins (HSC) encoded by constitutively active HSC70 (Liu et al. 2012). In the 70 kDa heat shock protein family, HSC70 is in the constitutively expressed form, which is actively expressed under non-stressed cells and remains unchanged or only slightly induced upon stressful stimuli, while HSP70 is highly induced during stress. HSC70 shares some of the structural and functional similarity with HSP70 and as molecular chaperon (Erbse et al. 2004; Liu et al. 2012). They play a crucial role in protein folding/unfolding, assembly/disassembly, degradation and translocation, and cellular protection against various stresses. In addition, HSC70 have also been implicated in defense response to microbial infections. HSC70 contain three domains such as an ATPase domain, a substrate-binding domain and a lid domain (Yan et al. 2010).

Antimicrobial peptides (AMPs) are major innate components of the immune system of invertebrates, vertebrates and plants against pathogens invasion. The new drugs have constantly been under investigation because of the increased development of new antibiotic-resistant bacteria (Hancock and Patrzykat 2002; Jiang et al. 2004; He et al. 2007). In recent years, naturally or designed AMPs are recognized as promising drug candidates due to their wide antimicrobial spectrum, modularity, low toxicity and decreased resistance development by target cell. All AMPs are generally small in size, membrane-active hydrophobic and positively charged molecules. The net positive charges increase their relative binding nature to microbial membrane which retains overall net negative charges. More investigation is focused on AMPs due to their high specificity to prokaryotic cells and low toxicity to eukaryotic cells (Sims et al. 1974; Nguyen et al. 2011; Sarika et al. 2012).

HSC70 and their isoforms have been cloned and characterized from various fish species and their different functions investigated against various stresses (Wang et al. 2015). However, to our knowledge no heat shock cognate proteins possess antimicrobial activity against pathogenic microorganisms. Recently, Taniguchi et al. (2013) derived three antimicrobial peptides from rice HSP70 that was found to have antimicrobial and membrane disruption activity. In this study, we have reported a complete molecular characterization of HSC70 which we identified from the cDNA library of *C. striatus* (*Cs*). The nucleotide and protein sequence of *Cs* HSC70 were analyzed using various biological computational tools. The temporal and spatial expression pattern of *Cs*HSC70 in response to fungal and bacterial infection was reported. We also determined the antimicrobial features of *Cs*HSC70 by synthesizing two peptides namely HSC70 A1 and HSC70 A2 from its amino terminal. For the first time, we report a *Cs*HSC70 derived cationic antimicrobial peptide HSC70 A1 that exhibited potent antimicrobial activity without hemolytic activity.

Materials and Methods

CsHSC70 Identification

Full length *Cs*HSC70 was identified from a cDNA library of *C. striatus* established using GS FLX™ technology. In short, cDNA library of *C. striatus* was developed using total RNA (Life Technologies, India), which was obtained from *C. striatus*. The total RNA was further purified into mRNA (Miltenyi Biotech, Germany) and then cDNA (Invitrogen, USA) was synthesized. The cDNA library was developed using Invitrogen (USA) kit and sequenced using GS FLX™ technology (Roche, India) as described in the company protocol. The detailed protocol of cDNA library development was reported in our earlier studies (Abirami et al. 2016; Prasanth et al. 2014; Rajesh et al. 2016). During Blast, a molecule encoded *Cs*HSC70 was identified from the library and considered for the present study.

In Silico Analysis

CsHSC70 Sequence

A putative open reading frame (ORF) and its corresponding amino acid sequence of *Cs*HSC70 cDNA was determined using Expasy Translate tool (Gasteiger et al. 2005). The physico-chemical properties of the *Cs*HSC70 polypeptide including number of amino acid residues, molecular weight, iso-electric point (pI), instability index and aliphatic index was analyzed using PROTPARAM online server (Gasteiger et al. 2005). Also, the *Cs*HSC70 was subjected to similarity search, which was performed through BLAST at NCBI Database. The analysis of secondary structural elements of *Cs*HSC70 was conducted in SOPMA (Geourjon and Deleage 1995). The motifs and domains of the *Cs*HSC70 were identified from PROSITE (de Castro et al. 2006), SMART (Letunic et al. 2015) and NCBI-CDD (Bauer et al. 2015) programs. Pairwise comparison and sequence alignments were carried out in Clustal W (ver. 2) (Thompson et al. 1994); further the alignment was edited in Bioedit (ver. 7.1.3.0) (Hall 1999). The evolutionary distance of *Cs*HSC70 was obtained from Poisson model phylogenetic tree construction; for this analysis we used neighbor joining (NJ) algorithm that was embedded in MEGA 5.05 with 5000 bootstrap repetitions (Koichiro et al. 2013). Three dimensional structures of *Cs*HSC70 proteins as

well as the *Cs*HSC70 A1 and *Cs*HSC70 A2 peptides were established through multiple-threading alignments with potential templates (Yang et al. 2015)on I-TASSER server. The established models were visualized in PyMOL (ver. 1.00) and RasMol programs. Ramachandran plot analysis was used for the validation of the 3D models (Lovell et al. 2002).

CsHSC70 A1 and CsHSC70 A2 Peptides

The antimicrobial features such as positive charge, hydrophobic residues and protein binding potentiality of predicted peptides were predicted on PepDraw and Antimicrobial Peptide Calculator and Predictor (APD2) programs. To develop the helical wheel structure of the predicted peptides *Cs*HSC70 A1 and *Cs*HSC70 A2, Schiffer–Edmundson (http://rzlab.ucr.edu/scripts/wheel/wheel.cgi) program was applied.

Synthesis of Peptides

*Cs*HSC70 derived analogs including HSC70 A1 and HSC70 A2 (Table 1) was synthesized by solid phase peptide synthesis method (SynPeptide Co., LTD, Shanghai, China). The peptides were further purified in reverse phase high-performance liquid chromatography (HPLC); and received the purity of 93.8 (HSC70 A1) and 97.1% (HSC70 A2). The molecular mass of the purified peptide analogs were confirmed by MALDI TOF-MS.

MBC of Peptide Analogs

We measured the minimum bactericidal concentration (MBC) of the two synthesized peptides against Gram-negative bacteria (*Aeromonas hydrophila* MTCC 1739, *Escherichia coli* ATCC 25922 and *Pseudomonas aeruginosa* ATCC 25668,) and Gram positive bacteria (*Bacillus mycoides* MTCC 8920, *Micrococcus luteus* MTCC 6164 and *Staphylococcus aureus* ATCC 25923). The MBC of peptides towards selected bacteria were estimated using the modified method of Clinical and Laboratory Standards Institute (CLSI) guidelines. The selected bacteria were grown in optimum media and culture conditions overnight and diluted into each well in a density of 1×10^6 CFU/ml. In brief, 100 µl of selected bacteria were pipetted into microtiter plate with different concentrations (20, 40, 80 and 160 µg/ml) of *Cs*HSC70 A1 and *Cs*HSC70 A2. A negative (DEPC treated nuclease-free deionized water) and positive (Ampicillin) control were also maintained. Then, the titer plate was incubated at 37 °C for 4 h; and the MBC (µg) was determined by absorbing the optical density (OD) at 600 nm in a micro plate reader.

Quantification of Hemolytic Activity

The hemolytic activity of *Cs*HSC70 A1 was measured according to the method described by Kumaresan et al. (2015). In short, red blood cells (RBCs) were collected from a volume of heparinized human blood (Ethical Clearance No. CDRI/IEC/2014/A1) by centrifugation at 2000×*g* for 5 min and washed thrice in PBS (pH 7.4) The cellular pellet was re-suspended in PBS and diluted about 4% (v/v). A 50 microliter of peptide solutions at various concentrations (20, 40, 80, 120 µg/ml) were further added and seeded in a 96-well plate. Along with this, 50 µl of 4% (v/v) Triton X-100 as positive control or 50 µl PBS as negative control was also incubated without agitation for one hat 37 °C. The hemolysis was measured by absorbance of the supernatant at 405 nm using a UV spectrophotometer (UV-1800, Shimadzu UV Spectrophotometer). The percentage of hemolysis was calculated as:

$$[(\text{Sample absorbance} - \text{Negative control})/(\text{Positive control} - \text{Negative control})] \times 100.$$

Scanning Electron Microscope (SEM) Observation

Micrococcus luteus cells were serially diluted at a density of 8×10^8 cells/ml in 200 µl of 10 mM PBS and the suspension was separated equally into two tubes. The *Cs*HSC70 A1 (40 µg/ml) sample was added into one tube and incubated at 30 °C for 24 h. The other tube was used as a control. After the incubation, treated cells were centrifuged at 5000×*g* for 10 min at 4 °C and the cells prefixed in 2.5% glutaraldehyde solution and 0.1 M Na-cacodylate buffer (pH 7.2) overnight at 4 °C for 1 h. Cells were washed with series of ethanol (30, 50, 70, 90 and 100%) for dehydration. The cells were dried in liquid CO_2 at a critical point. The samples were sputtered with gold using platinum coating

Table 1 Amino acid sequences and properties of the peptides used in the study

Peptide	*Cs*HSC70 A1	*Cs*HSC70 A2
Sequence	DNRMVN-HFISEFKRKYKK	RARFEELNADLFRG
Size (no. of amino acid)	18	14
Net charge	+4	0
Molecular mass (Da)	2340.7	1693.8
Hydrophobic ratio (%)	27	42
Protein-binding potential (Boman index)	3.98 kcal/mol	3.81 kcal/mol
pI	10.17	7.10

at 10 mA for 2 min. The morphology changes of *M. luteus* cells treated with *Cs*HSC70 A1 peptide were assessed using FEI Quanta FEG 200-High Resolution Scanning Electron Microscope.

Bacterial Cell Membrane Damage Induced by CsHSC70 A1

The membrane damage of *Cs*HSC70 A1 peptide to *M. luteus* cells was determined by detection of propidium iodide (PI) influx into cells as done previously by Kumaresan et al. (Kumaresan et al. 2015). *M. luteus* cells were cultured to mid log phase and diluted to density of $OD_{600} = 0.6$ in PBS. The *Cs*HSC70 A1 peptide (40 µg/ml) was treated with 200 µl of bacterial suspension and incubated at 37 °C for 20 min. Then, the cells were re-suspended in PI solution (5 µg/ml). The fluorescence signal in treated cells was determined by Fluorescence Assisted Cell Sorter Flow Cytometer (BD Biosciences) and analyzed with CELL-QUEST software.

Gene Expression Analysis

Animal Rearing

Healthy *C. striatus* with an average body weight ~50 g were received from Porurlake, Chennai, India and transported in plastic containers (50 l) to the aquaria at Division of Fisheries Biotechnology and Molecular Biology, Department of Biotechnology, SRM University, Kattankulathur. The transported individuals were acclimatized and maintained in the laboratory condition (temperature: 28 ± 1 °C and pH: 7.2 ± 0.2) as experimented in our earlier studies (Venkatesh et al. 2016; Rajesh et al. 2015; Prasanth et al. 2013; Abirami et al. 2013).

In Vivo Investigation on Immune Challenges

In order to determine the mRNA expression of *Cs*HSC70 against fungal, bacterial and other synthetic stimulants, *C. striatus* were injected with the biological [(i) fungus *Aphanomyces invadans*, a primary causative agent of epizootic ulcerative syndrome (EUS) in murrels and (ii) bacteria *Aeromonas hydrophila*, a secondary causative agent of EUS in murrels] and synthetic stimulant [(iii) Poly I:C (γ-irradiated, Sigma-Aldrich, India), polyinosinic-polycytidylic acid sodium salt, a synthetic analog of double-stranded RNA (dsRNA)] intraperitoneally. PBS (1×) was prepared and served as control (100 µl/50 g fish).

In fungus challenge, each individual received 100 µl of live *A. invadans* at a concentration of 10^2 spores suspended in 1× PBS. The isolation of *A. invadans* from EUS

infected fish was reported in our earlier studies (Prasanth et al. 2013; Abirami et al. 2013). In the bacterial challenge experiment, the fish received 100 µl of *A. hydrophila* per fish at a concentration of 5×10^6 CFU/ml suspended in 1× PBS. *A. hydrophila* was also isolated from EUS infected *C. striatus* muscle as reported by Dhanaraj et al. (2008). For viral analogue induction, poly I:C was injected (100 µl/50 g fish) to the fishes at a concentration of 150 µg/100 µl.

Tissue Sampling

To investigate the tissue expression of mRNA under normal physiological conditions, tissues including intestine, heart, liver, spleen, kidney, head kidney, brain, blood, gill, skin and muscle were collected from healthy individuals. Further, to study the defense responses of *Cs*HSC70, tissues with highest expression was sampled after being challenged with pathogens and other synthetic immune stimulants at 3, 6, 12, 24, 48 and 72 h post-injection. The obtained tissues were stored as per the protocol for total RNA extraction. Three fishes were sampled for each tissue at each time point of each challenge.

RNA Extraction and cDNA Synthesis

In order to amplify the cDNA of *Cs*HSC70, the total RNA was extracted from both the control and immune challenged fish using Tri Reagent™ method (Life Technologies, India). Invitrogen™ SuperScript™ VILO™ cDNA Synthesis Kit was used to synthesize *Cs*HSC70 cDNA from the total RNA isolated from the tissues. Approximately 2.5 µg/µl of total RNA was used for cDNA synthesis along with 5× VILO ™ Reaction Mix (4 µl), 10× SuperScript™ Enzyme Mix (2 µl) and DEPC treated water. The contents were mixed properly and incubated at 25 °C for 10 min and 42 °C for 60 min in PCR machine. The reaction was terminated by increasing the temperature to 85 °C for 5 min. Lastly, the acquired cDNA was kept at −20 °C until further use.

Spatial and Temporal Expression by qRT-PCR Program

Gene expression pattern of *Cs*HSC70 in different tissues from both healthy and challenged group was analyzed using Light Cycler 96 (Real Time PCR System, Roche Diagnostics GmbH, Germany). The primers designed for the study are *Cs*HSC70 F1 (GGG ACC ATA TCT GGG CTT AAT G) and *Cs*HSC70R2 (CAC CAC CCA GGT CAA AGA TAA G). The primers of the internal control β-actin are β-actin F3 (TCT TCC AGC CTT CCT TCC TTG GTA) and β-actin R4 (GAC GTC GCA CTT CAT GAT GCT GTT). The assay was conducted in a total volume of 20 µl

including diluted cDNA (template), SYBR® Green Mix, primers and double distilled water. We followed our standardized thermal cycle condition (Prasanth et al. 2013). The obtained data were analyzed with the program supplied along with the Roche instrument and the gene expression was calculated following the method of Livak and Schmittgenm (Livak and Schmittgenm 2001).

Statistics

All the data obtained from the study were subjected to one-way ANOVA followed by Tukey's Multiple Range Test (SPSS11.5).

Results

Identification and Analysis CsHSC70

*Cs*HSC70 sequence was identified from the cDNA library and deposited in GenBank database under the accession ID, HF955035. The nucleotide and derived amino acid sequences of *Cs*HSC70 are shown in E-supplementary data. The sequence comprises of 1953 base pairs (bp) nucleotides along with an open reading frame (ORF) of 650 amino acids. The predicted molecular weight of the sequence is 71.56 kDa and its theoretical isoelectric point is 5.2.

CsHSC70 Motif and Domain Analysis

The analysis revealed that *Cs*HSC70contained three HSP70 family signature motifs such as [9]IDLGTTYS[16,] [97]IFDLGGGTFDVSIL[110] and [333]IVLVGGSTRIPKIQK[347]. It also had three major functional domains including N-terminal ATPase domain (1–381), substrate binding domain (385–543) and C-terminal domain (537–620). The polypeptide contained acytoplasmic characteristic motif EEVD, a non-organellar stress protein motif RARFEEL and repeats of tetrapeptide (GGMP) at C terminal domain. Moreover, two bipartite nuclear localization signal motifs such as KK and RRLRT are present in the C-terminal, which is responsible for the translocation into the nucleus (Fig. 1). In addition, some high confidently predicted common motifs such as *N*-glycosylation site, *N*-myristoylation site, casein kinase II phosphorylation site, protein kinase C phosphorylation site and amidation site were also observed (E-suppl. data). In amino acid composition, the *Cs*HSC70 polypeptide chain is rich in residues including lysine, aspartic acid, alanine, glycine, leucine, isoleucine, threonine, valine, serine and glutamine, as predicted by DNAssist 2.2.

Homology and Phylogeny

Pair wise alignment revealed that *Cs*HSC70 shared 96% identity to mandarin fish, *Siniperca chuatsi* HSC70-2 and yellowtail, *Seriola quinqueradiata* HSC70-2 (data not shown). Multiple sequence alignment showed that cytoplasmic characteristic motif, non-organellar stress protein motif, putative bipartite nuclear localization signal motifs such as KK and RRLRT and repeats of tetrapeptidewere strongly conserved in *Cs*HSC70 (Fig. 1). Evolutionary relationship of the *Cs*HSC70 was performed along with the other HSC70reported from vertebrates (E-suppl. data). The phylogenetic tree diverged into two clades; fish and higher vertebrate HSC70. The fish HSC70 clade was further separated into HSC70-1 and HSC70-2 subgroups. *Cs*HSC70 was clustered together with HSC70-2 from *Siniperca chuatsi* and further grouped with HSC70-2 subgroup, which confirmed that *Cs*HSC70 belongs to HSC70-2 isoforms. The topology of the tree mainly reflected the taxonomic classification.

Structural Characterization

The minimum free energy (MFE) of the predicted mRNA structure of *Cs*HSC70 is -603.1 kcal/mol. The predicted mRNA structure showed that the mRNA is almost paired and very few nucleotides remain unpaired. The secondary structural elements of *Cs*HSC70 are 36.7% α-helix, 11.8% β-sheet and 51.3% random coil. Further, the tertiary structure of *Cs*HSC70 contained three functional domains including a 44 kDa amino-terminal adenosine triphosphatase (ATPase) domain, a 18 kDa substrate binding domain and a 10 kDa carboxyl-terminal domain (Fig. 2a). Ramachandran plot analysis was established to validate the 3D model and the results showed that 82.1% of amino acids exist in favored region, 10.3% in allowed region and 7.6% in outlier region.

Bioinformatics Analysis of CsHSC70 A1 and CsHSC70 A2 Peptides

On the basis of sequence, size, charge, charge distribution, helical propensity, hydrophobicity, amphipathicity or surface features and previous reports, we identified and derived two AMPs namely *Cs*HSC70 A1 and *Cs*HSC70 A2 from the N terminal of ATPase domain. Both AMPs were synthesized to analyze the antimicrobial properties. Both *Cs*HSC70 A1 and *Cs*HSC70 A2 were found to have a linear α-helical structure (Fig. 2b). *Cs*HSC70 A1 showed antimicrobial properties including remarkably high positive charge (+4), hydrophobic residues (27%) and protein binding potential (3.98 kcal/mol) analyzed by PepDraw and Antimicrobial Peptide Calculator and
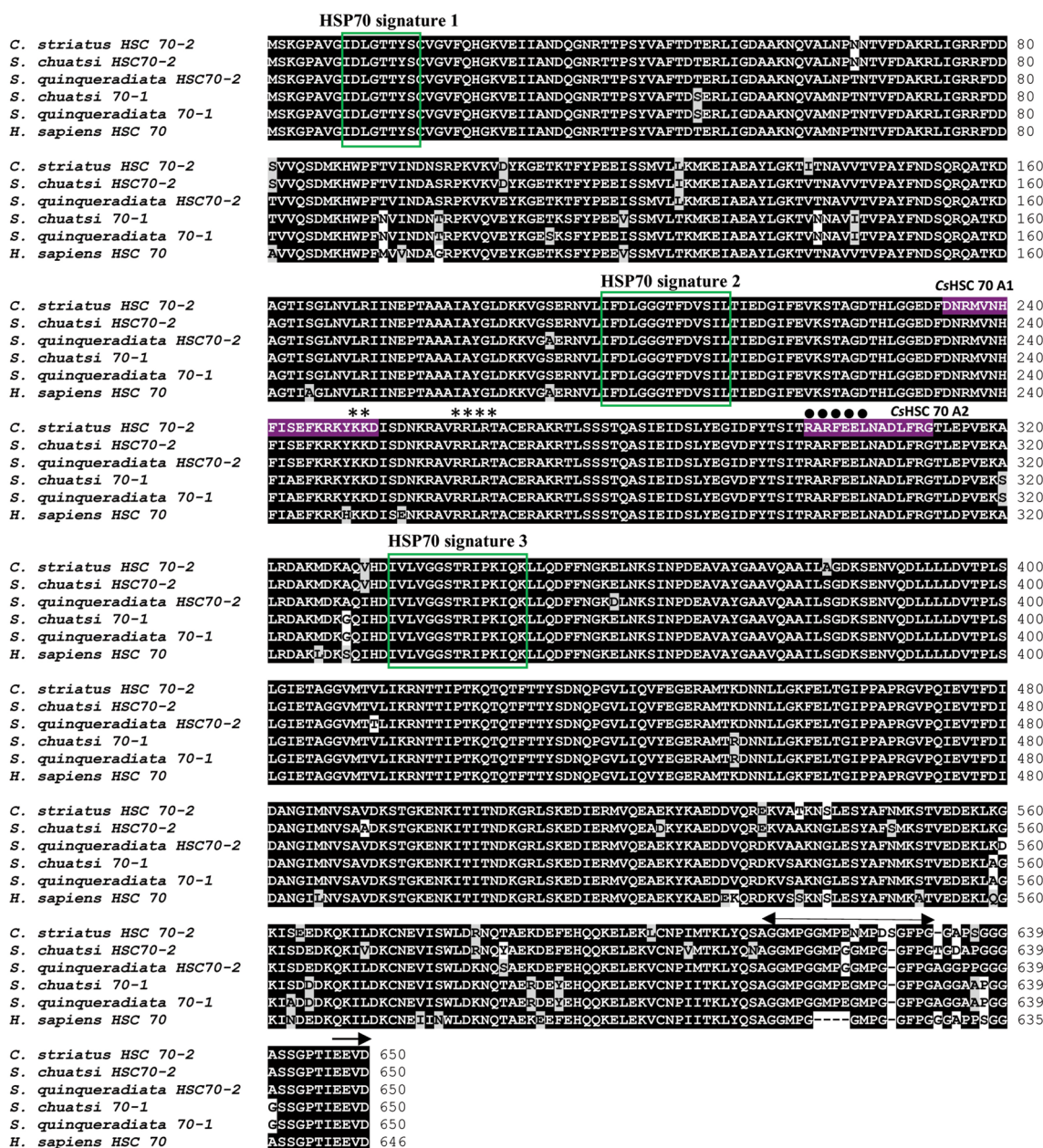
Fig. 1 Multiple sequence alignment of *Cs*HSC70 with its orthologs: *Siniperca chuatsi* HSC70-2 (AGS83420), *Seriola quinqueradiata* HSC70-2 (BAG82849), *S. chuatsi* HSC70-1 (AGS83421), *S. quinqueradiata* HSC70-1 (BAG82848) and *Homo sapiens* HSC70 (BAD96505). The *Cs*HSC70 containing Hsp70 family signature motifs which are enclosed in *rectangular boxes*. The C terminal EEVD motif was shown in *single arrow underlined* over the sequence. The non-organellar motif RARFEEL is indicated by *block spot* above the residues, and the putative bipartite nuclear localization signals, KK and RRLRT, are mentioned by '*' above the sequence. The repeats of the tetrapeptide (GGMP) located in the C terminal region are underlined by *double arrow* over the sequence. The derived antimicrobial peptides are *shaded* in *pink color*. (Color figure online)

Predictor (APD2). Moreover, the analysis showed that the amino acid percentage of *Cs*HSC70 A1 was found to be rich in lysine and arginine. The predicted molecular weight of *Cs*HSC70 A1 was 2340 Daltons. Similarly, *Cs*HSC70 A2 contains 42% hydrophobic residues and its protein binding potential was 3.81 kcal/mol. However, it is interesting to note that *Cs*HSC70 A2 does not hold

any charge (Table 1). Schiffer–Edmundson helical wheel modeling was used to predict amphipathic nature of both *Cs*HSC70 A1 and *Cs*HSC70 A2 (Fig. 3a, b). The wheel model showed that the peptides are linear α-helical molecule bearing both hydrophobic and hydrophilic residues on the opposing sides.
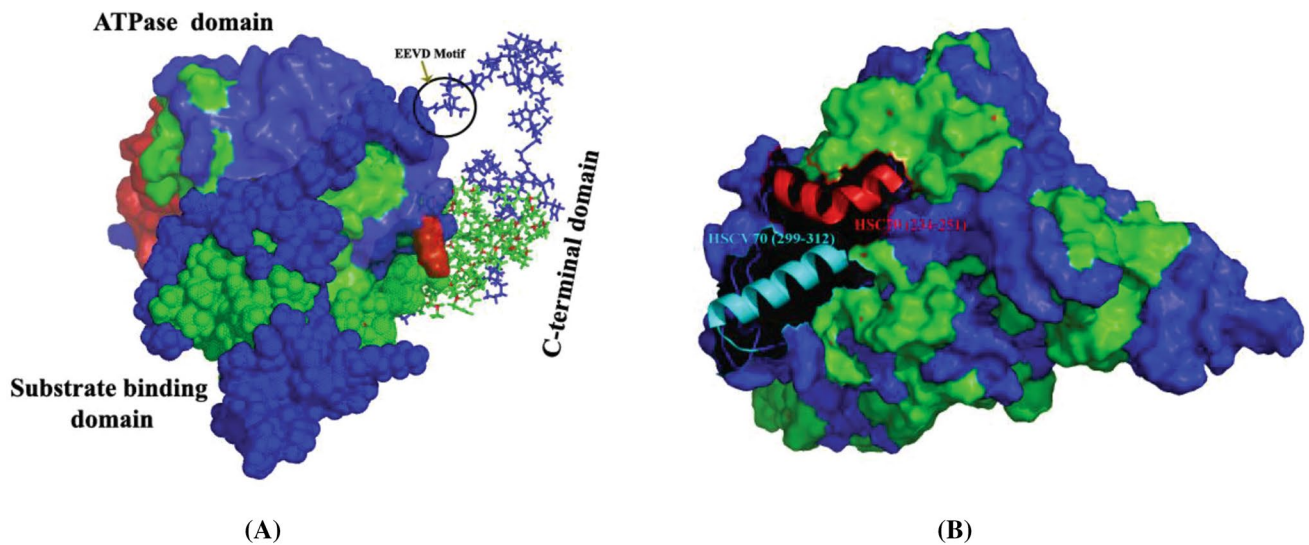
Fig. 2 Predicted 3D structure of *Cs*HSC70 (**a**) and secondary structure of peptides (**b**): *Cs*HSC70 A1 and *Cs*HSC70 A2 derived from *Cs*HSC70 established using PyMol software
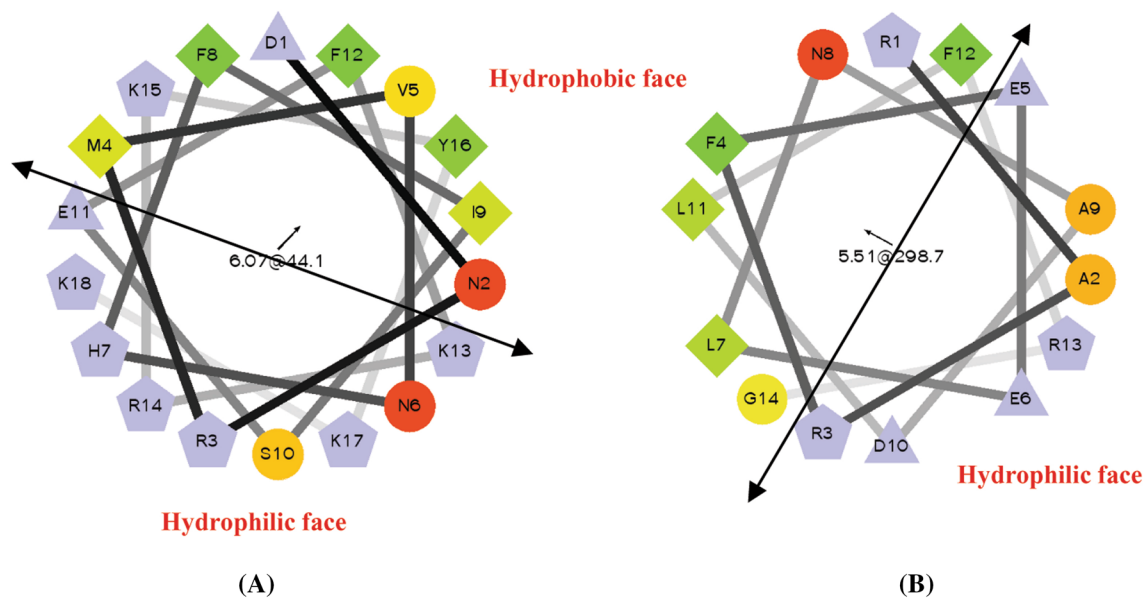

Fig. 3 Schiffer–Edmundson helical wheel diagram showing probable amphipathic conformation of *Cs*HSC70 derived antimicrobial peptides: *Cs*HSC70 A1 (**a**) and *Cs*HSC70 A2 (**b**)

Bactericidal Activity

The bactericidal activity of the two peptides was determined by measuring minimal bactericidal concentrations (MBCs) against Gram-negative bacteria and Gram positive bacteria. Among the two, *Cs*HSC70 A1 exhibited potent growth-inhibitory activity against Gram-positive bacteria, *M. luteus* (40 µg/ml) than other bacteria tested.

In the case of *Cs*HSC70 A2, it showed very low activity against *M. luteus* only at higher concentration (>160 µg/ml), whereas no significant activity was observed against other microorganisms tested.

Therefore, considering the potent activity of *Cs*HSC70 A1 on the bactericidal activity, it was chosen for further assays including hemolytic assay, cell damage and membrane disruption ability.

Hemolytic Activity of CsHSC70 A1

Hemolytic activity of *Cs*HSC70 A1 at various concentrations (20, 40, 80 and 160 µg) was determined in human RBCs. The peptide analog did not show any hemolytic activity even at a concentration of 160 µg/ml. Moreover, no difference in hemolysis was observed between *Cs*HSC70 A1 treated RBCs and PBS treated RBCs, whereas triton X-100 showed the maximum hemolytic activity (Fig. 4).

Scanning Electron Microscopic (SEM) Observation

The morphological alteration of *M. luteus* cells treated with *Cs*HSC70 A1 was determined under SEM (Fig. 5). Comparing the treated and untreated *M. luteus* cells under SEM, the treated cells appeared to be damaged and there was a significant destructive effect noticed which was affecting the integrity of *M. luteus* cells. Moreover, the outer membrane was apparently affected due to the treatment of *Cs*HSC70 A1. Also, the treated cells become deformed in morphology with partial lack of cytoplasmic membrane. The cytoplasm of the peptide treated cells tends to spill out of the cell and ultimately lead to cell death.

Membrane Disruption Ability

Membrane disruption activity of *Cs*HSC70 A1 on *M. luteus* cell membrane was determined by treating the cells with the peptide. Since PI dye is impermeable to live cells; it can be used to detect the dead cells in population. The PI can bind with DNA by intercalating between the base pairs. Hence, the cells were stained with PI and the cell morphology was determined using a flow cytometer. The assay indicated that 99.6% of cells exhibited no signal when it was not treated with peptide, whereas the PI fluorescence signal was observed when the cells were treated for nearly

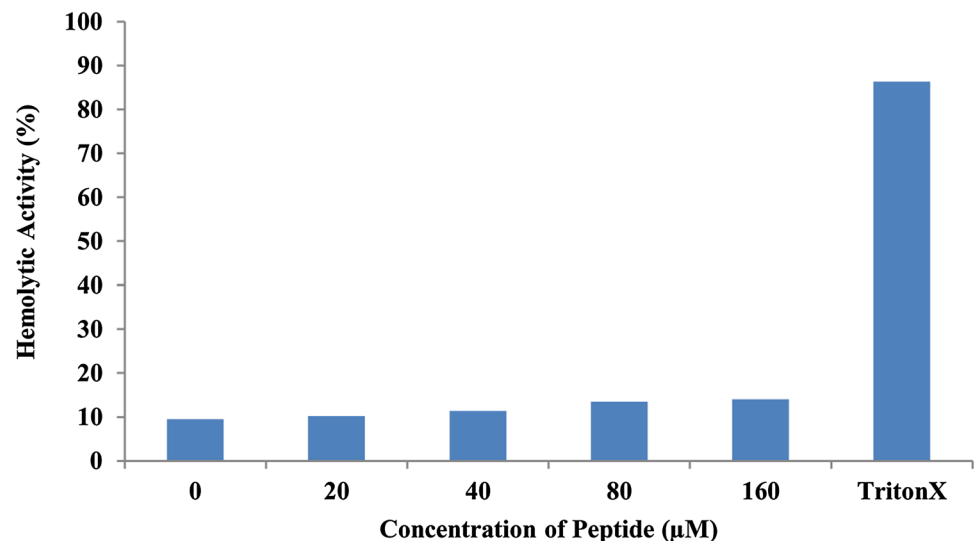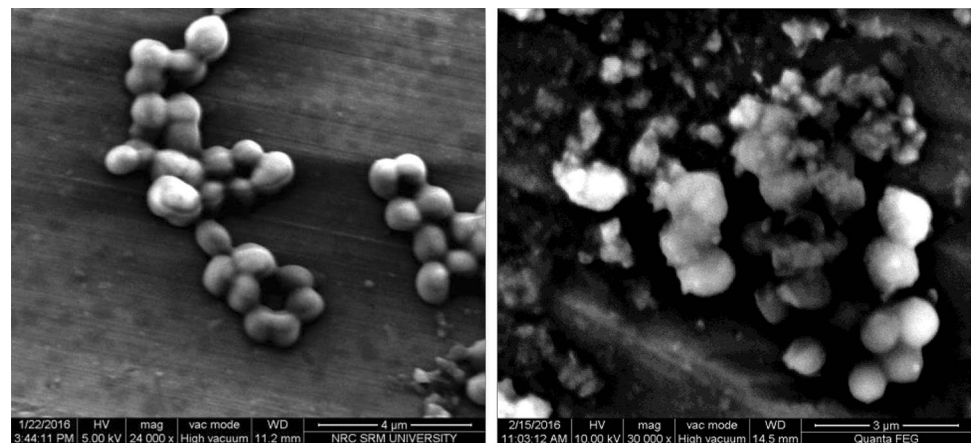**Fig. 4** Hemolytic activity of *Cs*HSC70 A1 peptide on human RBCs

Fig. 5 Scanning electron microscope image of *M. luteus* after treatment with *Cs*HSC70 A1

Untreated cells   **Treated cells**

20 min with peptide at a concentration of 40 μM/ml. When the cells were treated with peptide for 50 min, the percentage of cells with PI was about 38% (Fig. 6). The intensity
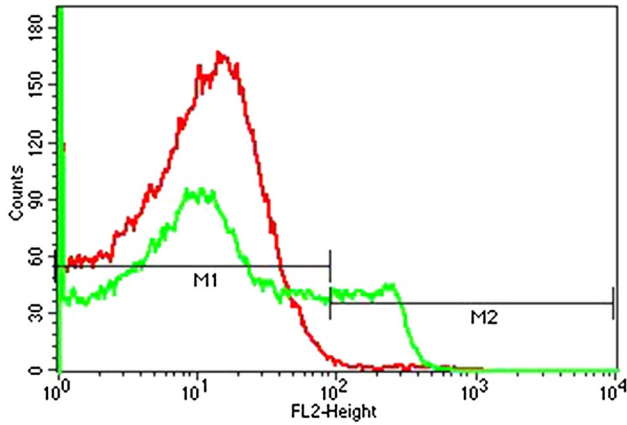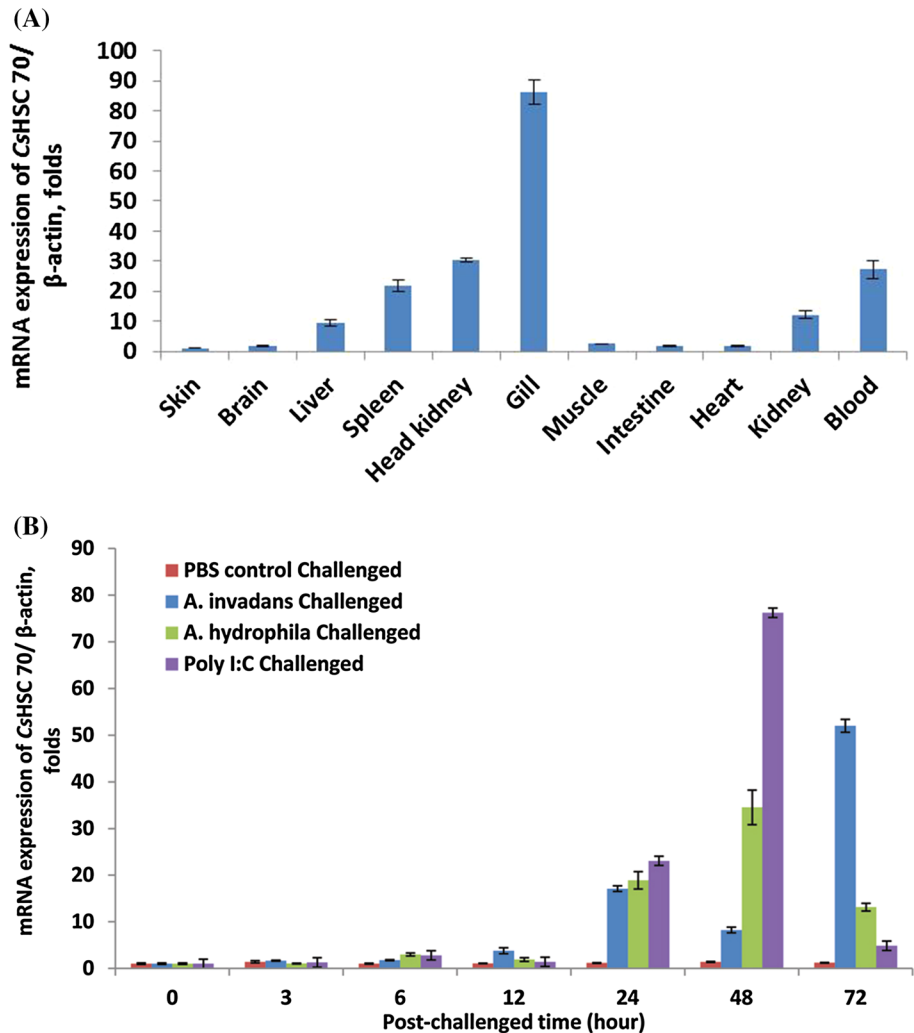

Fig. 6 Effect of *Cs*HSC70 A1 peptide treatment on *M. luteus* cell membrane disruption. (Color figure online)

of fluorescence increased as the concentration of the peptide increased.

Pathogen Challenge and Gene Expression of CsHSC70

Using real time PCR, relative expression of *Cs*HSC70 mRNA was observed in all the tissues using β-actin as an internal control (Fig. 7a). However, significant expression of *Cs*HSC70 mRNA transcripts was found in gill, to a lesser extent in head kidney, blood, spleen and liver and at low level in other tissues. Therefore, gill was chosen for further study on the possible roles of *Cs*HSC70 mRNA regulation upon fungal, bacterial, and poly I:C stimulant. In *A. invadans* infected tissue, *Cs*HSC70 expression was considerably up-regulated at 72 h post stimulation (P < 0.05) (Fig. 7b), whereas in *A. hydrophila*, it was significantly (P < 0.05) up-regulated at 48 h post stimulation compared to their respective controls (Fig. 7b). In poly I:C stimulated case, the expression level of *Cs*HSC70 was started

Fig. 7 Relative quantification of *Cs*HSC70 gene expression. **a** Results of tissue distribution analysis of *Cs*HSC70. Data are given as a ratio to *Cs*HSC70 mRNA expression in skin. **b** The time course of *Cs*HSC70 mRNA expression in gills at 0, 3, 6, 12, 24, 48 and 72 h post-injection with *A. invadans, A. hydrophila* and poly I:C. (Color figure online)

to up-regulate during 24 h (Fig. 7b) and reached its peak (P < 0.05) at 48 h post-stimulation.

Discussion

HSC70 is the most important member of the HSP70 family, and it is constitutively expressed under non-stressed cells. It remains unchanged or slightly inducible upon stimulation. HSC70 also showed some similarity with HSP70 in structural and functional properties. Nevertheless, in comparison with HSP70 and other heat shock family members, HSC70 bears numerous unique properties. It regulates plenty of cellular functions through interaction with co-chaperones and many other molecules. It also entails in both innate and adaptive immunity including antigen presentation, T cell receptor complex formation, autoimmunity and tumor immunity and also implicates in various diseases (Liu et al. 2012; Erbse et al. 2004). It may become a biomarker for diagnosis and potential therapeutic targets for design, discovery and development of novel drugs to treat various diseases.

The *Cs*HSC70-1 cDNA sequence was 1953 bp in length along with a 1950 bp ORF which encodes a poly peptide length of 650 amino acids. The amino acid sequence was highly homologous with its counterparts of other fish species. The sequence possesses three canonical signatures and major functional domains similar to eukaryotic HSP70 family. The non-organellar stress protein motif RARFEEL and the regulatory motif EEVD of cytoplasmic characteristic are present at the C-terminal of *Cs*HSC70 and located in the cell cytosol and cytoplasm. The EEVD motif is strongly conserved in all eukaryotic HSC70 and other members of HSP70 family. The motif is vital for association with some co-chaperones (Demand et al. 1998; Lo et al. 2004). The putative bipartite nuclear localization signals, KK and RRLRT found in the*Cs*HSC70 are most essential for selective translocation into nucleus (Demand et al. 1998; Liu et al. 2004).

The amino acid sequence of *Cs*HSC70 showed a high sequence identity (96%) with HSC70-2 from *S. chuatsi* and *S. quinqueradiata*. The multiple sequence alignment of *Cs*HSC70 with orthologous from fish and other members of HSC70 family revealed that *Cs*HSC70 was strongly conserved (92%). Evolutionary tree classified the HSC70 into two clade; lower vertebrate (fish) and higher vertebrate HSC70s. The fish HSC70 clade was further divided into HSC70-1 and HSC70-2 as subgroup. This similar divergence was supported by Wang et al. 2015 and Yabu et al. 2011. *Cs*HSC70 reported in this study is closely related to *S. chuatsi* HSC70-2. Plenty of HSC70 isoform were said to be existing in an individual genome (Liu et al. 2012). However, those different isoforms were only described in fish

species including rainbow trout, zebrafish, common carp, walking catfish, yellowtail and tilapia.

The predicted mRNA structure showed that the mRNA is almost paired and very few nucleotides remain unpaired. The predicted mRNA structure of *Cs*HSC70 along with its MFE value attempts to show that the mRNA of *Cs*HSC70 is strongly stable. Xiong and Waterman (1997) discussed that the MFE of mRNA secondary structure based on the pairing of nucleotides. Further, they (Xiong and Waterman 1997) described that if the bases are paired they have negative value and if unpaired they have positive value. In this case, *Cs*HSC70 mRNA had −603.1 kcal/mol, so, it is implied that the *Cs*HSC70 mRNA has a stable structure. The total secondary structural content of *Cs*HSC70 was 36.7% α-helix, 11.8% β-sheet and 51.3% random coil. The rich presence of random coil elements makes the tertiary structure of *Cs*HSC70 unstructured. As in human HSC70 (Smith et al. 1998; Tsukahara et al. 2000; Sullivan et al. 2000), the tertiary structure of *Cs*HSC70 protein is also predicted to have three functional domains including a 44 kDa amino-terminal adenosine triphosphatase (ATPase) domain, a 18 kDa substrate binding domain and a 10 kDa carboxyl-terminal domain. It is well known that HSC70 is an ATP binding chaperone, thus HSC70 showed the ATPase activity; by which it can bind and hydrolyze ATP into ADP and results in a conformational change of HSC70 and further caused substrate binding (Sullivan et al. 2000). The protein folding activity of HSC70 relies on their binding ability to expose hydrophobic amino acid sequence of the protein substrates which is regulated by ATP. The regulatory motif EEVD at the C terminal is completely conserved in HSC70 and HSP70 family members of all eukaryotes and it is the most crucial factor for association with some co-chaperones (Mosser et al. 2000).

On the basis of surface features, charges and secondary structure, two novel α-helical AMPs*Cs*HSC70 A1 and *Cs*HSC70 A2 were derived from *Cs*HSC70 protein. To identify the peptides, the amino acids residues present on the surface of the *Cs*HSC70 protein amino terminal ATPase domain were examined. The surface features were chosen because they comprise both hydrophilic and hydrophobic amino acids that make amphipathic nature which is most important for AMPs. Structural or physical parameters studies on AMPs showed numerous factors including sequence, size, charge, charge distribution, helical propensity, hydrophobicity, amphipathicity and angles subtended by hydrophobic and hydrophilic faces of the helix which control the antimicrobial activity (Giangaspero et al. 2001). *Cs*HSC70 A1 exhibited better growth-inhibitory activity against *M. luteus*in lower concentration, whereas *Cs*HSC70 A2 exhibited very low activity at higher concentration. Therefore, from the analysis it is confirmed that *Cs*HSC70 A1 was superior to *Cs*HSC70 A2 in hindering the growth

of the pathogen. A reasonable question may arise here why the *Cs*HSC70 A2 peptide showed very low antimicrobial activity only at higher concentration even though the peptide has amphipathicity and helical propensity; it may due to the peptide having no net charge. Also, it may due to the absence of post-translational modification in the peptide.

 *Cs*HSC70 A1 peptide showed better bactericidal activity without any hemolytic activity. There was no significant difference in hemolysis between *Cs*HSC70 A1 and PBS treated RBCs. Hence, *Cs*HSC70 A1 is considered to be a potent and safe AMP candidate for use against *M. luteus*. As PI dye is impermeable to live cells; it can generally be used for identifying cells with membrane damage in a population. The PI can bind with DNA by intercalating between the base pairs (Joshi et al. 2010; Li et al. 2013; Park and Lee 2009). Flow cytometric analysis was employed to quantitatively determine the membrane damage induced by the addition of *Cs*HSC70 A1 to *M. luteus* cells. Using the technique, we found that the percentages of *M. luteus* cells stained with PI increased in a concentration dependent manner. The activity of *Cs*HSC70 A1 against *M. luteus* was mostly due to the membrane-destabilizing ability.

The SEM observation demonstrated that *Cs*HSC70 A1 could cause significant morphological damage to the treated bacterial cells. Treated cells appeared to be damaged and a significant destructive effect occurred that affects the integrity of *M. luteus* cells. The outer membrane structure is apparently affected and the cells become deformed morphologically with partial lack of cytoplasmic membrane. The cytoplasm of the cells tends to spill out of the cell and lead to death. The damage to the *M. luteus* cell wall and cytoplasmic membrane may cause loss of structural integrity which results in loss of cell content and cell death. Nevertheless, several probable mechanisms of AMPs against various microorganisms were proposed. Buforin II inhibits *E. coli* growth by means of penetrating the cell membranes and binding to DNA and RNA of cells and another AMP known as magainin 2 deters bacterial growth by forming pores on the cell membrane; despite both AMPs being linear α-helical amphipathic in nature (Park et al. 1998; Matsuzaki et al. 1997). On the basis of the obtained results, we could propose that the mode of action of *Cs*HSC70 A1 could be akin to either buforin or magainin 2 peptide reported previously.

The expression of *Cs*HSC70 mRNA transcripts could be detected in all the tested tissues with different expression levels. The obviously abundant *Cs*HSC70 transcripts were observed in gill which was significantly higher than that in other tissues. So, compared with other tissues, gill may be more sensitive to stressful challenges. Also, it may due to gill being the respiratory organ and having direct contact with external or aquatic environment. The highest level of transcripts in gill proposed that *Cs*HSC70 is used as a

sensitive biomarker for different classes of environmental assault. The results of our study are in agreement with the earlier reports of Zhang et al. (2011) and Poompoung et al. (2014) who observed the expression of HSC70 and HSP70 in immune tissues including gills, head kidney, spleen and blood of grass. Moreover, it is worthwhile to note that the highest levels of *Cs*HSC70 transcripts in gills may correlate with the osmotic regulation in striped murrel.

Accordingly, expression profiles of *Cs*HSC70 mRNA were examined in response to challenge of *A. invadans, A. hydrophila* and poly I:C induction using snakehead murrel gill as a cell model. In *A. invadans* infected tissue, *Cs*HSC70 expression was considerably up-regulated at 72 h post stimulation. After poly I:C treatment, the expression level of *Cs*HSC70 was started to up-regulate during 24 h and reached its peak at 48 h post infection. The moderate and down-regulation of *Cs*HSC70 till 48 and 72 h post-infection of viral analog and fungal challenge suggests that the expression was seriously affected by both fungus and viral analog immunostimulant. Fungus primarily activates the host innate immune molecules through binding between PAMPs and host pattern recognition molecules (PRRs). Fungal virulent factors or PAMPs are complex carbohydrates which in turn make the pathogen-host interaction more complex which could be responsible for delayed activation of host innate immune responses (Sorrell and Chen 2009).

Upon *A. hydrophila* challenge, *Cs*HSC70 was started to slightly up-regulate at 6, 24 h post challenge and peaked at 48 h post challenge compared to their respective control. The expression of HSC70-2 transcripts in the gills of walking catfish slightly increased after injection with *A. hydrophila* at 24 h. It was likely that *Cs*HSC70 was insensitive to the bacteria at the early hours following injection. Bacterial infection differentially induced the expression of HSC70s in liver, gills, brain and skeletal muscle of walking catfish during 48 h. The temporal expression level of HSC70s upon *A. hydrophila* infection varies from organ to organ. The HSC70-2 mRNA concentrations peaked at 24 h and decreased to level of the control at 48 h in liver of walking catfish, instead,the HSC70-2 mRNA level peaked at 48 h skeletal muscle (Poompoung et al. 2014). Few more studies show that bacterial infection regulates the HSC/HSP70 mRNA transcripts in *S. ocellatus* (Dang et al. 2010), channel catfish (Elibol-Flemming et al. 2009), Wuchang bream (Ming et al. 2009) and Pacific abalone (Cheng et al. 2007). These findings not only revealed that HSC/HSP70 is entailed in fish immune response, but also provoked us to examine the expression patterns of HSC70 in fish immune cells to understand their roles in fish immunity. Virus also induces the heat shock response in fish and shellfishes. Reports showed that the modulation of HSP90 expression at 6, 12, 24, 48, and 72 h post infection upon

nodavirus-infection in grouper fish (Chen et al. 2010). Further, Huang et al. (2008) reported that the expression of HSP21 was down-regulated upon WSSV infection in shrimp. All together, the reports showed the potential involvement of HSP/HSC against viral infection, which has been proved in our case also.

In summary, we report a complete molecular characterization of *Cs*HSC70 which we identified from the cDNA library of *C. striatus*. The temporal and spatial expression pattern of *Cs*HSC70 was determined in response to fungal, bacterial and viral analog stimulation. The nucleotide and protein sequence was analyzed using various computational tools. We also determined the antimicrobial features including bactericidal, hemolytic, cellular damage and membrane disruption activities of *Cs*HSC70 A1 and *Cs*HSC70 A1 peptides synthesized from amino terminal of the *Cs*HSC70 protein sequence. Further works on the determination of the molecular mode of antimicrobial action of *Cs*HSC70 A1 and *Cs*HSC70 A2 has to be elucidated.

Compliance with Ethical Standards

Conflict of interest Akila Sathyamoorthi, Rajesh Palanisamy, Mariadhas Valan Arasu, Naif Abdullah Al-Dhabi, Mukesh Pasupuleti and Jesu Arockiaraj declare that they have no conflict of interest.

Research Involving Human and Animal Rights The animals used in this study were treated with care following the ethical procedures of the University guidelines and regulations. All experimental protocols were approved by the university research committee of SRM University. The use of human blood was approved by the ethics committee at SRM University (361/IEC/2012) and CSIR-CDRI, Lucknow (Ethical Clearance No. CDRI/IEC/2014/A1).

Informed Consent Informed consent was obtained from the donors before collecting the blood.

References

Abirami A, Venkatesh K, Akila S, Rajesh P, Prabha N, Prasanth B, Roy A, Thirumalai MK, Gnanam AJ, Pasupuleti M, Marimuthu K, Arockiaraj J (2013) Fish lily type lectin-1 contains β-prism 2 architecture: immunological characterization. Mol Immunol 56(4):497–506

Abirami A, Venkatesh K, Akila S, Mariadhas VA, Naif AA, Arockiaraj J (2016) Coagulation profile, gene expression and bioinformatics characterization of coagulation factor X of striped murrel *Channa striatus*. Fish Shellfish Immunol 55:149–158

Bauer AM, Derbyshire MK, Gonzales NR, Lu S, Chitsaz F, Geer LY, Geer RC, He J, Gwadz M, Hurwitz DI, Lanczycki CJ, Lu F, Marchler GH, Song JS, Thanki N, Wang Z, Yamashita RA, Zhang D, Zheng C, Bryant SH (2015) CDD: NCBI's conserved domain database. Nucleic Acids Res 43:222–226

Chen YM, Kuo CE, Wang TY, Shie PS, Wang WC, Huang SL, Tsai TJ, Chen PP, Chen JC, Chen TY (2010) Cloning of an orange-spotted grouper *Epinephelus coioides* heat shock protein 90AB (HSP90AB) and characterization of its expression in response to nodavirus. Fish Shellfish Immunol 28:895–904

Cheng PZ, Liu X, Zhang GF, He JG (2007) Cloning and expression analysis of a HSP70 gene from pacific abalone (*Haliotis discus hannai*). Fish Shellfish Immunol 22:77–87

Dang W, Hu YH, Zhang M, Sun L (2010) Identification and molecular analysis of a stress inducible Hsp70 from *Sciaenopsocellatus*. Fish Shellfish Immunol 29:600–607

de Castro CJ, Sigrist A, Gattiker V, Bulliard PS, Langendijk-Genevaux E, Gasteiger E, Bairoch A, Hulo N (2006) ScanProsite: detection of PROSITE signature matches and ProRule-associated functional and structural residues in proteins. Nucleic Acids Res 34:362–365

Demand J, Luders J, Hohfeld J (1998) Thecarboxy-terminal domain of Hsc70 provides binding sites for a distinct set of chaperone cofactors. Mol Cell Biol 18:2023–2028

Dhanaraj M, Haniffa MA, Ramakrishnan CM, Singh SVA (2008) Microbial flora from the epizootic ulcerative syndrome (EUS) infected murrel *Channa striatus* (Bloch, 1797) in Tirunelveli region. Turk J Vet Anim Sci 32:221–224

Elibol-Flemming B, Waldbieser GC, Wolters WR, Boyle CR, Hauson L (2009) Expression analysis of selected immune-relevant genes in channel catfish during *Edwardsiella ictaluri* infection. J Aquat Anim Health 21:23–35

Erbse A, Mayer MP, Bukau B (2004) Mechanism of substrate recognition by Hsp70 chaperones. Biochem Soc Trans 32:617–621

Gasteiger E, Hoogland C, Gattiker A, Duvaud S, Wilkins MR, Appel RD, Bairoch A (2005) Protein identification and analysis tools on the ExPASy server. In: Walker JM (ed) The proteomics protocols handbook. Humana Press, Totowa, pp 571–607

Geourjon C, Deleage G (1995) SOPMA: significant improvements in protein secondary structure prediction by consensus prediction from multiple alignments. Comput Appl Biosci 11:681–684

Giangaspero A, Sandri L, Tossi A (2001) Amphipathic alpha helical antimicrobial peptides. Eur J Biochem 268:5589–5600

Hall TA (1999) BioEdit: a user-friendly biological sequence alignment editor and analysis program for Windows 95/98/NT. Nucl Acids Symp Ser 41:95–98

Hancock REW, Patrzykat A (2002) Clinical development of cationic antimicrobial peptides, from natural to novel antibiotics. Curr Drug Targets 2:79–83

He J, Eckert R, Pharm T, Simanian MD, Hu C, Yarbrough DK, Qi F, Anderson MH, Shi W (2007) Novel synthetic antimicrobial peptides against *Streptococcus mutans*. Antimicrob Agents Chemother 51:1351–1358

Huang PY, Kang ST, Chen WY, Hsu TC, Lo CF, Liu KF, Chen LL (2008) Identification of the small heat shock protein, HSP21, of shrimp *Penaeus monodon* and the gene expression of HSP21 is inactivated after white spot syndrome virus (WSSV) infection. Fish Shellfish Immunol 25:250–257

Jiang S, Hong Z, Guo W, Xiaoyun, G, Gengfa, L, Yongning L, Guangxia X (2004) A synthetic peptide derived from bactericidal/permeability-increasing protein neutralizes endotoxin in vitro and in vivo. Int Immunopharmacol 4:527–537

Joshi S, Bisht GS, Rawat DS, Kumar A, kumar R, Maiti S, Pasha S (2010) Interaction studies novel cell selective antimicrobial peptides with model membranes and *E. coli* ATCC 11775. Biochim Biophys Acta 1798:1864–1875

Koichiro T, Glen S, Daniel P, Alan F, Sudhir K (2013) MEGA6: molecular evolutionary genetics analysis version 6.0. Mol Biol Evol 30:2725–2729

Kumaresan V, Bhatt P, Ganesh MR, Harikrishnan R, Arasu M, Al-Dhabi NA, Pasupuleti M, Marimuthu K, Arockiaraj J (2015) A novel antimicrobial peptide derived from fish goose type lysozyme disrupts the membrane of *Salmonella enterica*. Mol Immunol 68:421–433

Letunic I, Doerks T, Bork P (2015) SMART: recent updates, new developments and status in 2015. Nucl Acids Res 43:257–260

Li L, Shi YH, Cheserek MJ, Su GF, Le GW (2013) Antibacterial activity and dual mechanisms of peptide analog derived from cell-penetrating peptide against *Salmonella typhimurium* and *Streptococcus pyogenes*. Appl Microbial Biotechnol 97:1711–1723

Liu J, Yang WJ, Zhu XJ, Karouna-Renier NK, Rao RK (2004) Molecular cloning and expression of two HSP70 genes in the prawn, *Macrobrachiumrosenbergii*. Cell Stress Chaperon 9: 313–323

Liu T, Daniels CK, Cao S (2012) Comprehensive review on the HSC70 functions, interactions with related molecules and involvement in clinical diseases and therapeutic potential. Pharmacol Ther 136:354–374

Livak KJ, Schmittgenm TD (2001) Analysis of relative gene expression data using real-time quantitative PCR and the 2(-Delta Delta C (T)) method. Methods 25:402–408

Lo WY, Liu KF, Liao IC, Song YL (2004) Cloning and molecular characterization of heat shock cognate 70 from tiger shrimp (*Penaeus monodon*). Cell Stress Chaperon 9:332–343

Lovell SC, Davis IW, Arendall WB III, de Bakker PI W, Word JM, Prisant MG, Richardson JS, Richardson DC (2002) Structure validation by Calpha RAMPAGE: Ramachandran plot assessment geometry: phi, psi and C beta deviation. Proteins 50:437450

Matsuzaki K, Sugishita K, Harada M, Fujii N, Miyajima K (1997) Interactions of an antibacterial peptide, magainin 2, with outer and inner membranes of Gram negative bacteria. Biochim Biophys Acta 1327:119–130

Ming JH, Xie J, Xu P, Liu WB, Ge XP, Liu B, He Y, Cheng Y, Zhou Q, Pan L (2009) Molecular cloning and expression of two HSP70 genes in the Wuchang bream (*Megalobrama amblvcenhala Yih*). Fish Shellfish Immunol 28:407–418

Mosser DD, Caron AW, Bourget L, Meriin AB, Sherman MY, Morimoto RI, Massie B (2000) The chaperone function of hsp70 is required for protection against stress-induced apoptosis. Mol Cell Biol 20:7146–7159

Nguyen LT, Haney EF, Vogel HJ (2011) The expanding scope of antimicrobial peptide strutures and their modes of action. Trends Biotechnol 29:464–472

Park C, Lee DG (2009) Fungicidal effect of antimicrobial peptide arenicin-1. Biochim Biophys Acta 1788:1790–1796

Park CB, Kim HS, Kim SC (1998) Mechanism of action of the antimicrobial peptide buforin II: buforin II kills microorganisms by penetrating the cell membrane and inhibiting cellular functions. Biochem Biophys Res Commun 244:253–257

Poompoung P, Panprommin D, Srisapoome P, Poompuang S (2014) Cloning and expression of two HSC70 genes in walking catfish *Clarias macrocephalus* (Günther, 1864) challenged with *Aeromonas hydrophila*. Aqua Res 45:1319–1331

Prasanth B, Venkatesh K, Rajesh P, Chaurasia MK, Gnanam AJ, Mukesh P, Arockiaraj J (2013) Immunological role of C4 CC chemokine-1 from snakehead murrel *Channa striatus*. Mol Immunol 57:292–301

Prasanth B, Mukesh CK, Rajesh P, Venkatesh K, Abirami A, Sathyamoorthi A, Gnanam AJ, Kasi M, Pasupuleti M, Ramaswamy H, Arockiaraj J (2014) Molecular cloning, characterization and gene expression of murrel CXC chemokine receptor 3a against sodium nitrite acute toxicity and microbial pathogens. Fish Shellfish Immunol 30:245–253

Rajesh P, Venkatesh K, Harikrishnan R, Arasu MV, Al-Dhabi NA, Arockiaraj J (2015) Functional roles and gene regulation of tumor necrosis factor receptor 1 in freshwater striped murrel. Mol Immunol 66:240–252

Rajesh P, Prasanth B, Venkatesh K, Mukesh P, Arockiaraj J (2016) Innate and adaptive immune molecules of striped murrel *Channa striatus*. Rev Aquacult. doi:10.1111/raq.12161

Roberts RJ, AgiusC, Saliba C, Bossier P, Sung YY (2010) Heat shock proteins (chaperones) in fish and shellfish and their potential role in relation to fish health: a review. J Fish Dis 33:789–801

Sarika, Iquebal MA, Rai A (2012) Biotic stress resistance in agriculture through antimicrobial peptides. Peptides 36:322–330

Sims PJ, Waggoner AS, Wang CH, Hoffman JF (1974) Studies on the mechanism by which cyanine dyes measure membrane potential in red blood cells and phosphatidylcholine vesicles. BioChemistry 13:3315–3330

Smith DF, Whitesell L, Katsanis E (1998) Molecular chaperones: biology and prospects for pharmacological intervention. Pharmacol Rev 50:493–513

Sorrell TC, Chen SC (2009) Fungal-derived immune modulating molecules. Adv Exp Med Biol 666:108–120

Sullivan CS, Cantalupo P, Pipas JM (2000) The molecular chaperone activity of simian virus 40 large T antigen is required to disrupt Rb-E2F family complexes by an ATP-dependent mechanism. Mol Cell Biol 20:6233–6243

Taniguchi M, Ikeda A, Nakamichi S, Ishiyama Y, Saitoh E, Kato T, Ochiai A, Tanaka T (2013) Antimicrobial activity and mechanism of action of a novel cationic α-helical octadecapeptide derived from heat shock protein 70 of rice. Peptides 48:147–155

Thompson JD, Higgins DG, Gibson TJ (1994) CLUSTAL W: improving the sensitivity of progressive multiple sequence alignment through sequence weighting, position-specific gap penalties and weight matrix choice. Nucleic Acids Res 22:4673–4680

Tsukahara F, Yoshioka T, Muraki T (2000) Molecular and functional characterization of HSC54, a novel variant of human heat-shock cognate protein 70. Mol Pharmacol 58:1257–1263

Venkatesh K, Gayathri R, Faizal N, Dhayanithi NB, Arasu MV, Al-Dhabi NA, Harikrishnan R, Arockiaraj J (2016) Multifunctional murrelcaspase 1, 2, 3, 8 and 9: conservation, uniqueness and their pathogen-induced expression pattern. Fish Shellfish Immunol 49:493–504

Wang P, Xua P, Zeng S, Zhou L, Zeng L, Li G (2015) Comparative analysis of sequence feature and expression of two heat shock cognate 70 genes in mandarin fish *Siniperca chuatsi*. Gene 560:26–36

Xiong M, Waterman MS (1997) A phase transition for the minimum free energy of secondary structures of a random RNA. Adv Appl Math 18:111–132

Yabu T, Imamura S, Mohammed MS, TouhataK, Minami T, Terayama M, Yamashita M (2011) Differential gene expression of HSC70/HSP70 in yellowtail cells in response to chaperone-mediated autophagy. FEBS J 278:673–685

Yamashita M, Yabu T, Ojima N (2010) Stress protein HSP70 in fish. Aqua Bio Sci Monogr 3:111–141

Yan F, Xia D, Hu J, Yuan H, Zou T, Zhou Q, Liang L, Qi Y, Xu H (2010) Heat shock cognate protein 70 gene is required for prevention of apoptosis induced by WSSV infection. Arch Virol 155:1077–1083

Yang J, Yan R, Roy A, Xu D, Poisson J, Zhang Y (2015) I-TASSER suite: protein structure and function prediction. Nat Methods 12:7–8

Zhang A, Zhou X, Wang X, Zhou H (2011) Characterization of two heat shock proteins (Hsp70/Hsc70) from grass carp (*Ctenopharyngodon idella*): evidence for their differential gene expression, protein synthesis and secretion in LPS-challenged peripheral blood lymphocytes. Comp Biochem Physiol Part B 159:109–114